PHYSICAL REVIEW B **93**, 241109(R) (2016)

Magnetic excitations in the $S = \frac{1}{2}$ antiferromagnetic-ferromagnetic chain compound $BaCu_2V_2O_8$ at zero and finite temperature

E. S. Klyushina,[1,2,*] A. C. Tiegel,[3] B. Fauseweh,[4] A. T. M. N. Islam,[1] J. T. Park,[5] B. Klemke,[1] A. Honecker,[6] G. S. Uhrig,[4] S. R. Manmana,[3] and B. Lake[1,2]

[1]*Helmholtz-Zentrum Berlin für Materialien und Energie, 14109 Berlin, Germany*

[2]*Institut für Festkörperphysik, Technische Universität Berlin, 10623 Berlin, Germany*

[3]*Institut für Theoretische Physik, Georg-August-Universität Göttingen, 37077 Göttingen, Germany*

[4]*Lehrstuhl für Theoretische Physik I, Technische Universität Dortmund, 44221 Dortmund, Germany*

[5]*Heinz Maier-Leibnitz Zentrum, TU München, 85747 Garching, Germany*

[6]*Laboratoire de Physique Théorique et Modélisation, CNRS UMR 8089, Université de Cergy-Pontoise, 95302 Cergy-Pontoise Cedex, France*

(Received 19 February 2016; published 20 June 2016)

Unlike most quantum systems which rapidly become incoherent as temperature is raised, strong correlations persist at elevated temperatures in $S = \frac{1}{2}$ dimer magnets, as revealed by the unusual asymmetric line shape of their excitations at finite temperatures. Here, we quantitatively explore and parametrize the strongly correlated magnetic excitations at finite temperatures using high-resolution inelastic neutron scattering of the model compound $BaCu_2V_2O_8$ which we show to be an alternating antiferromagnetic-ferromagnetic spin-$\frac{1}{2}$ chain. Comparison to state of the art computational techniques shows excellent agreement over a wide temperature range. Our findings hence demonstrate the possibility to quantitatively predict coherent behavior at elevated temperatures in quantum magnets.

DOI: 10.1103/PhysRevB.93.241109

In the study of unconventional states of matter, quantum magnetic materials with their strong correlations play a crucial role [1–5]. Quantum mechanical coherence and entanglement are intrinsic to these systems, both being relevant for potential applications in quantum devices [6,7]. However, the question arises for their persistence when increasing temperature. Intuitively, one expects temperature to suppress quantum behavior, as typically encountered in the study of quantum criticality [8]. Interestingly, this is not always the case, and in certain systems, e.g., in the presence of disorder, coherent behavior is not simply suppressed by temperature, but rather an interesting interplay develops [9,10], which can lead to counterintuitive behavior such as the increase of conductance through molecules with temperature [11].

Another example is the extraordinary coherence of certain magnetic excitations at elevated temperatures. This was theoretically predicted for one-dimensional (1D) gapped quantum dimer antiferromagnets (AFMs) by using integrable quantum field theory [12] and was experimentally confirmed on the strongly dimerized spin-$\frac{1}{2}$ AFM alternating chain compound copper nitrate, which has a spin-singlet ground state and gapped triplet excitations (henceforth referred to as triplons [13]) confined within a narrow band [14]. Here, the triplons interact strongly via the AFM interdimer coupling and also via an effective repulsive interaction due to the hard-core constraint. The resulting strong correlations lead to the experimentally observed asymmetric broadening of the line shape with temperature [14,15]. So far, such experimental data were compared to exact diagonalization data from small systems and to results using a low-temperature expansion around the strongly dimerized limit of Heisenberg spin-$\frac{1}{2}$ chains [16,17]. Further experimental studies revealed that the strongly correlated behavior at elevated temperatures is not restricted to 1D systems. It was recently observed that the line shape in the three-dimensional (3D) coupled-dimer antiferromagnet $Sr_3Cr_2O_8$ also becomes asymmetric and increasingly weighted towards the center of the band as temperature increases [18,19]. So far, no reliable theoretical approaches on the microscopic level are available which capture large systems beyond the limit of strong dimerization. The development of such techniques is crucial to provide a quantitative description of the strongly correlated behavior at finite temperatures.

The scope of this Rapid Communication is to report the comparison of two currently developed theoretical approaches with quantitative predictive power to experimental data. These approaches are based on matrix product states (MPS) or density-matrix renormalization group (DMRG) techniques [20–22] and on the diagrammatic Brückner approach on top of continuous unitary transformations (DBA-CUT) [23,24], respectively. They provide an accurate description for the strongly correlated behavior of the magnetic excitations at finite temperatures in the dimer compound $BaCu_2V_2O_8$. High-resolution inelastic neutron scattering (INS) measurements are compared with these theoretical approaches. The analysis of the experimental and theoretical results reveals accurate quantitative agreement between the experimentally observed and the theoretically predicted strongly correlated behavior at finite temperature. This is our first key result. Because the couplings in $BaCu_2V_2O_8$ have been strongly debated in the literature, our second key result is to deduce the Hamiltonian of this compound and show that it is a highly dimerized antiferromagnetic-ferromagetic chain correcting the long-held view that the interdimer coupling is AFM or negligible. This observation implies our third key result, that the presence of strongly correlated behavior in gapped dimer systems is independent on the sign of the interdimer coupling.

*ekaterina.klyushina@helmholtz-berlin.de

 ©2016 American Physical Society

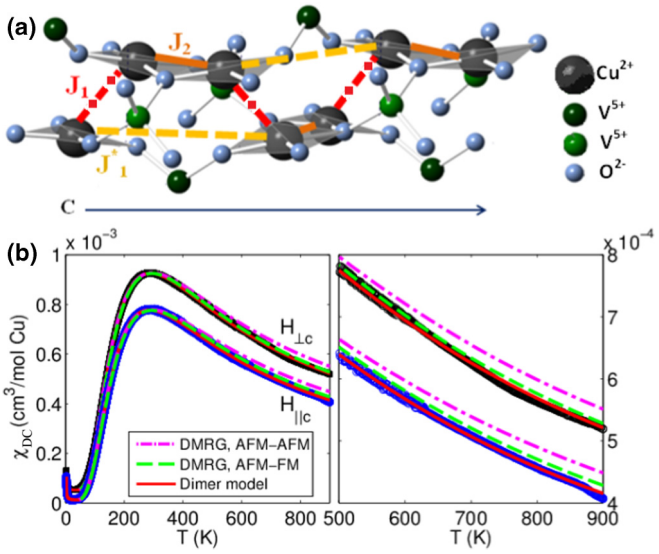

FIG. 1. (a) Crystal structure of $BaCu_2V_2O_8$ (the Ba^{2+} are omitted) showing the two proposed models of the dimerized chain arrangement along the c axis: the first model with exchange paths J_1^* (dashed line) and J_2 (solid line) resulting in two independent noninteracting dimerized linear chains [25]; the second model with exchange paths J_1 (dashed-dotted line) and J_2 (solid line) leading to a single dimerized screw chain [26]. (b) χ_{DC} as a function of temperature for a 1 T magnetic field applied parallel and perpendicular to the c axis. The solid line is the coupled-dimer model [27,28] where the g factors and exchange constants were fitted ($J_{intra} = 39.8 \pm 0.13$ meV, $J_{inter} = -9.87 \pm 2.64$ meV, $g_{||c} = 2.09$, $g_{\perp c} = 2.27$). The dashed and dashed-dotted lines are DMRG results with the exchange constants fixed to the values for the AFM-AFM and AFM-FM models, respectively; only the g factors were fitted. All fits included additional terms to account for paramagnetic impurities and van Vleck susceptibility. The AFM-FM model yields an anisotropic g factor $g_{||c} = 2.14 \pm 0.015$ and $g_{\perp c} = 2.29 \pm 0.015$. In $BaCu_2V_2O_8$ the plaquettes contain the c axis and rotate about it; $g_{||\text{plaquette}} = g_{||c} = 2.12 \pm 0.03$ and $g_{\perp\text{plaquette}} = 2g_{\perp c} - g_{||c} = 2.44 \pm 0.03$, in agreement with other cuprates with square-planar coordination [29–33].

Crystal structure. $BaCu_2V_2O_8$ has a tetragonal crystal structure (space group $I\bar{4}2d$, lattice parameters $a = b = 12.744$ Å, $c = 8.148$ Å). The magnetic Cu^{2+} ions ($S = \frac{1}{2}$) are coordinated by O^{2-} ions in square-planar geometry and these CuO_4 plaquettes form edge-sharing pairs Cu_2O_6 which rotate about the c axis and are oriented with the c axis lying within the plaquettes [Fig. 1(a)]. Previous constant-field magnetic susceptibility (χ_{DC}) [25,34–36], specific heat [25], and ^{51}V nuclear magnetic resonance [36,37] measurements revealed a nonmagnetic ground state with excitations above a gap of size $\Delta \approx 31.0$–40.5 meV. This implies that the Cu^{2+} ions are coupled into dimers by a dominant AFM intradimer interaction (J_{intra}), resulting in a spin-singlet ground state and gapped triplon excitations. The interdimer interaction (J_{inter}) was previously assumed to be AFM with strength between 0% and 20% of the intradimer coupling [25,34–37].

The exchange paths responsible for the J_{intra} and J_{inter} coupling are strongly debated in the literature [25,26,34,35]. Two models for $BaCu_2V_2O_8$ have been suggested [Fig. 1(a)]. The first, which assumes the paths J_2 and J_1^*, gives rise to almost straight independent noninteracting dimerized double chains parallel to the c axis [25]. The second, which consists of J_1 and J_2, couples the Cu^{2+} ions into a single alternating screw chain [26]. Both suggest that the AFM J_{inter} arises via the superexchange path J_2 (Cu-O-Cu) [26] between the two Cu^{2+} ions within the edge-sharing plaquettes while the J_{intra} is realized via the AFM supersuperexchange path J_1 or J_1^* (Cu-O-V-O-Cu) [26]. The second model is favored by two band structure investigations which predict that J_1 and J_2 are both AFM with ratio J_2/J_1 of 0.16 [26] or 0.05 [35], while J_1^* is much weaker.

Methods. Single crystals of $BaCu_2V_2O_8$ were grown in the Crystal Laboratory at the Helmholtz Zentrum Berlin für Materialien und Energie (HZB), using the traveling-solvent-floating-zone method [38]. χ_{DC} was measured using a superconducting quantum interference device at the Laboratory for Magnetic Measurements, HZB, over the temperature range 2–900 K. Single crystal INS measurements were performed on the thermal triple-axis spectrometer PUMA [39]. The magnetic excitation spectrum was mapped out at $T = 5$ K using a double-focused pyrolytic graphite (PG(002)) monochromator and analyzer with a fixed final wave vector $k_f = 2.662$ Å^{-1} giving an energy resolution of 2 meV. The line shape of the excitations was measured at the dispersion minima (6,0,1) and (8,0,0), for temperatures in the range of 3.5–200 K using a double-focused Cu(220) monochromator and PG(002) analyzer with fixed $k_f = 1.97$ Å^{-1} to give a higher energy resolution of 0.74 meV. The excitation spectra of $BaCu_2V_2O_8$ were calculated in the frequency domain using DMRG-based Chebyshev expansions [40] at zero [41–43] and finite temperature [44,45], taking into account the positions of the Cu^{2+} ions [46]. At finite temperature, this approach is combined with linear prediction [47,48]. The diagrammatic Brückner approach was used to compute the thermal fluctuations of the strongly interacting hard-core bosons on top of the effective model obtained by a continuous unitary transformation (DBA-CUT) [23,24,46]. Both calculations were performed for the $S = \frac{1}{2}$ alternating chain Heisenberg Hamiltonian

$$H = \sum_i J_{\text{intra}} \mathbf{S}_{i,1} \cdot \mathbf{S}_{i,2} + J_{\text{inter}} \mathbf{S}_{i,2} \cdot \mathbf{S}_{i+1,1}. \qquad (1)$$

Deducing the Hamiltonian. Figures 2(a) and 2(b) present INS data measured in the $(H,0,L)$ plane at $T = 5$ K. The magnetic excitation spectrum consists of two gapped branches which disperse along the L direction over the energy band 35.37 ± 0.05 meV to 45.56 ± 0.05 meV but are dispersionless along the H and K directions. The modes have the same periodicity and bandwidth, but are shifted with respect to each other by half a period and alternate in intensity. These results reveal that $BaCu_2V_2O_8$ is a highly dimerized 1D magnet where the dimers are coupled to form alternating chains along the c axis while the coupling within the ab plane is absent or negligibly small. The presence of a structure factor with two modes implies that these chains are not straight. Each mode is well reproduced by the one-triplon dispersion of an alternating chain [50,51] assuming that either both interactions are AFM [dashed line in Fig. 2(a)] or AFM and FM [solid line, Fig. 2(a)]. The extracted value of the alternating chain periodicity ($d = 4.04 \pm 0.04$ Å) is the same for both modes and is half the c lattice parameter. This periodicity corresponds

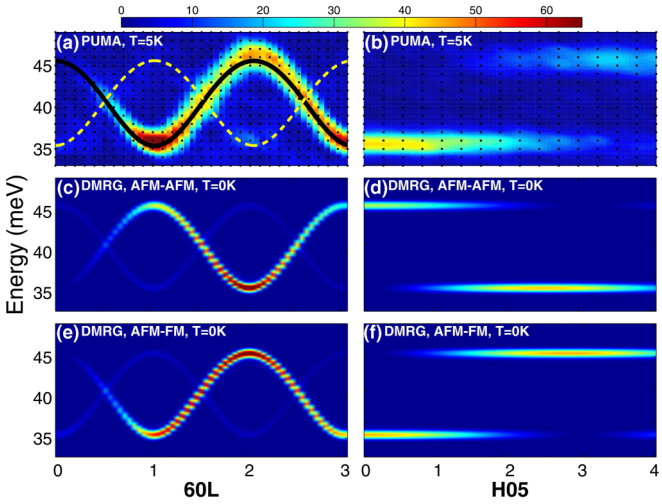

FIG. 2. Background-subtracted INS data along (a) $(6,0,L)$ and (b) $(H,0,5)$. The dashed and solid lines show the one-triplon dispersion to fifth order for the J_1-J_2 model with AFM-AFM ($J_1 = 40.75$ meV, $J_2 = 9.16$ meV) and AFM-FM ($J_1 = 40.92$ meV, $J_2 = -11.97$ meV) interactions, respectively. DMRG results for the dynamic structure factor for the J_1-J_2 model with AFM-AFM interactions along (c) $(6,0,L)$ and (d) $(H,0,5)$, and AFM-FM interactions along (e) $(6,0,L)$ and (f) $(H,0,5)$. The anisotropic magnetic form factor of the Cu^{2+} ions is taken into account [49] and a resolution broadening is included.

to the alternating screw chain model (J_1-J_2), while the linear chain model ($J_1^*-J_2$) can be excluded because it would have a periodicity of $d = c = 8.148$ Å. Assuming that both the J_{intra} and J_{inter} interactions are AFM, high-resolution energy scans at the dispersion minima and maxima were fitted using the fifth-order expansion of the alternating chain dispersion [50] and give the solution $J_{\text{intra}} = 40.75 \pm 0.02$ meV and $J_{\text{inter}} = 9.16 \pm 0.1$ meV. Equally good agreement was achieved for the AFM-FM model with exchange constants $J_{\text{intra}} = 40.92 \pm 0.01$ meV and $J_{\text{inter}} = -11.97 \pm 0.1$ meV [46].

To distinguish between the alternating AFM-AFM and AFM-FM screw chain models, DMRG computations of the magnetic excitation spectra were performed. The results for the $(6,0,L)$ and $(H,0,5)$ directions at zero temperature are shown for the AFM-AFM [Figs. 2(c) and 2(d)] and AFM-FM [Figs. 2(e) and 2(f)] models. In both cases gapped modes are predicted, matching the experimental data in terms of energy and periodicity. However, only the AFM-FM model agrees with the observed intensity while the AFM-AFM chain is clearly wrong since the intensities of the two modes are interchanged with respect to the experiment.

Static magnetic susceptibility verifies this result. Figure 1(b) shows the measured χ_{DC} for a magnetic field applied parallel and perpendicular to the c axis. While these two directions have similar features, they have different amplitudes because of the anisotropic g factor of Cu^{2+} in this compound (caption of Fig. 1). DMRG calculations of χ_{DC} were performed with the intrachain exchange constants fixed to the values obtained for the AFM-AFM and AFM-FM models. Best agreement is found for the AFM-FM model, confirming the FM nature of the interdimer interaction. In addition, the coupled-dimer model [28,30] was fitted to the data by varying the exchange constants and yields $J_{\text{intra}} = 39.8 \pm 0.13$ meV and $J_{\text{inter}} = -9.87 \pm 2.64$ meV, again confirming the AFM-FM model.

Our results reveal that $BaCu_2V_2O_8$ is an $S = \frac{1}{2}$ alternating screw chain with exchange paths J_1 and J_2, as predicted by band structure calculations [26,35]. However, in contrast to these predictions and to previous experimental work [25,34,36,37] which assumed both interactions to be AFM, we demonstrate that the weaker interdimer coupling is FM. While we cannot determine which of the two exchange paths is FM, it is most likely that $J_1 = J_{\text{intra}}$ is AFM, while $J_2 = J_{\text{inter}}$ is FM. Indeed, band structure calculations predict that the super-superexchange path J_1 provides the strongest AFM interaction [26,35] while the bridge angle of the J_2 Cu-O-Cu path is 94° and is close to the crossover from AFM to FM according to the Goodenough-Kanamori-Anderson rules [52–54].

Strongly correlated behavior. Now we turn to the question of whether $BaCu_2V_2O_8$ hosts also strongly correlated behavior at elevated temperatures. The alternating AFM-FM chain has received little experimental or theoretical attention since feasible physical realizations are rare. Thus, $BaCu_2V_2O_8$ provides the opportunity to investigate the effect of temperature on this kind of dimer system. This is achieved by performing energy scans at several temperatures up to 200 K (Fig. 3) at the dispersion minima ((6,0,1) and (8,0,0)) where the deviations from symmetric Lorentzian behavior are most pronounced. Figure 3 shows that the excitations broaden with increasing temperature, and at the highest temperatures the line shape appears asymmetric and weighted towards the center of the band. By fitting the data at 175 and 200 K to a symmetric Lorentzian $L(W_L, E)$ (where W_L is the width and E energy) convolved with the asymmetric instrumental resolution function $R(E)$ given by the line shape at a base temperature [solid red line in Fig. 3(a)], it is immediately clear that the line shape of the excitations at these temperatures does not have the symmetric Lorentzian profile represented by the dotted red line in Figs. 3(e) and 3(f).

In order to capture the asymmetry, the conventional width W_L in the Lorentzian function was replaced by $(W_L \rightarrow W_L + \alpha(E - E_0))$ where a finite α makes the line shape asymmetric about the peak position E_0. Thus the new fitting function $F(E)$ is

$$F(E) = A \cdot L(W_L + \alpha(E - E_0), E) * R(E). \qquad (2)$$

Here, A denotes the peak intensity. The solid red lines in Figs. 3(b)–3(f) present our best fits of $F(E)$ to the experimental data and reveal that the line shape of the excitations is asymmetric even down to 100 K. Figures 3(g) and 3(h) display the extracted values of W_L and of the asymmetry parameter α as a function of temperature and show that both increase with temperature.

Comparison with theory. To verify the experimentally observed asymmetric thermal line-shape broadening, we now compare it to theoretical results obtained by DMRG and DBA-CUT at finite temperatures for the AFM-FM model. Both approaches take account of the Gaussian resolution broadening but not of the asymmetry in the resolution function observed in the experiment. The DMRG results at $T = 100$,

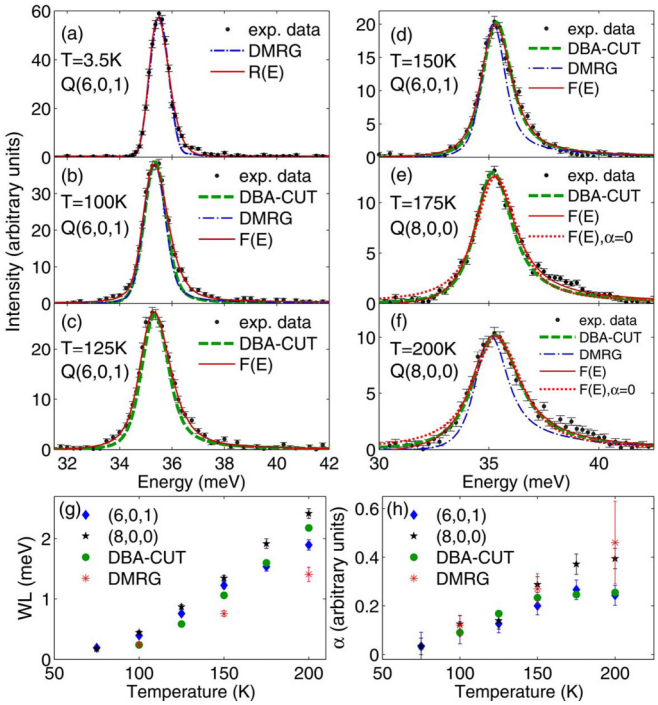

FIG. 3. Background-subtracted constant wave-vector scans at (6,0,1) and (8,0,0) measured at (a) $T = 3.5$ K, (b) $T = 100$ K, (c) $T = 125$ K, (d) $T = 150$ K, (e) $T = 175$ K, and (f) $T = 200$ K. At $T = 3.5$ K the excitations are resolution limited and the solid line gives the fit of the Gaussian function $R(E) = G(W_G + \beta(E - E_0), E)$ where the Gaussian width W_G has been replaced by $W_G \rightarrow W_G + \beta(E - E_0)$, which reproduces the asymmetric instrumental resolution function for finite β [46]. At other temperatures the solid and dotted lines correspond to the fits of Eq. (2) with α varied and $\alpha = 0$, respectively. The dashed and dashed-dotted lines are results from DBA-CUT and DMRG for the AFM-FM model, respectively. (g) and (h) show the temperature dependence of W_L and α from fitting the experimental data and theoretical results.

150, and 200 K reproduce the experimental data in Figs. 3(b), 3(d), and 3(f) (dashed-dotted blue line) assuming that the intradimer coupling changes slightly as temperature increases [46]. The dashed green line in Figs. 3(b)–3(f) represents the dynamic structure factors computed by DBA-CUT for 100, 125, 150, 175, and 200 K. Because the DBA-CUT peak positions are slightly offset from the experimental peaks at elevated temperatures [46], they were shifted for comparison to the experimental line shapes. Both techniques clearly predict asymmetric line-shape broadening weighted towards higher energies at finite temperatures. These two very different theoretical approaches are in good quantitative agreement, with the DBA-CUT approach better able to resolve the line shape, while the DMRG obtains the peak position better [46]. When fitting the theoretical results using $F(E)$ and taking into account their resolution functions [46], we extract the temperature dependence of W_L and α as plotted in Figs. 3(g) and 3(h), showing good quantitative agreement with the experiment. This confirms the persistence of correlation effects in this system at elevated temperatures, and in addition shows that this effect is independent of the sign of the interdimer exchange coupling (see the Supplemental Material [46] for a comparison of line shapes of AFM-AFM and AFM-FM models).

Summary. Combining recently developed theoretical approaches and high-precision inelastic neutron scattering, we quantitatively described the strongly correlated behavior at elevated temperatures in the 1D gapped dimer magnet $BaCu_2V_2O_8$ up to relatively high temperatures. Based on a customized fitting function, the asymmetry could be reliably captured and parametrized. Our first key result is the very good agreement between the experimentally observed and the theoretically computed line shapes obtained by the DMRG and the DBA-CUT approach, which demonstrates accurate prediction of coherent behavior in quantum magnets. In this way, one can identify strongly correlated systems which retain their coherence at elevated temperatures. Our second key result is that we unambiguously established the relevant Hamiltonian of $BaCu_2V_2O_9$, revealing that it is a rare example of an alternating AFM-FM chain and correcting previous results which assumed it to be an alternating AFM-AFM chain or an isolated dimer system [25,26,35–37]. This finding implies our third key result, that strong correlations in dimerized quantum magnets at elevated temperatures are independent of the sign of the interdimer exchange coupling. Equipped with these techniques and insights, we anticipate future investigations to explore how strongly correlated behavior depends quantitatively on relevant parameters such as the dimensions of the system, the size of the spins, and the statistics of the elementary excitations.

We would like to thank our late colleague Thomas Pruschke for his support of this project and useful discussions. This work is based upon experiments performed at the PUMA instrument operated by FRM II at the Heinz Maier-Leibnitz Zentrum (MLZ), Garching, Germany. We acknowledge the Helmholtz Gemeinschaft for funding via the Helmholtz Virtual Institute (Project No. VH-VI-521) and CRC/SFB 1073 (Project No. B03) of the Deutsche Forschungsgemeinschaft. We also thank D. A. Tennant and D. L. Quintero-Castro for helpful discussions.

[1] L. Balents, Nature (London) **464**, 199 (2010).

[2] *Frustrated Spin Systems*, edited by H. T. Diep (World Scientific, Singapore, 2013).

[3] *Introduction to Frustrated Magnetism*, edited by C. Lacroix, P. Mendels, and F. Mila, Springer Series in Solid-State Sciences Vol. 164 (Springer, Berlin, 2011).

[4] *Quantum Magnetism*, edited by U. Schollwöck, J. Richter, D. Farnell, and R. Bishop, Lecture Notes in Physics Vol. 645 (Springer, Berlin, 2004).

[5] P. Fazekas, *Lecture Notes on Electron Correlation and Magnetism*, Series in Modern Condensed Matter Physics Vol. 5 (World Scientific, Singapore, 1999).

[6] L. Amico, R. Fazio, A. Osterloh, and V. Vedral, Rev. Mod. Phys. **80**, 517 (2008).
[7] M. Nielsen and I. Chuang, *Quantum Computation and Quantum Information* (Cambridge University Press, Cambridge, U.K., 2000).
[8] S. Sachdev, *Quantum Phase Transitions*, 2nd ed. (Cambridge University Press, Cambridge, U.K., 2011).
[9] I. L. Aleiner, B. L. Altshuler, and G. V. Shlyapnikov, Nat. Phys. **6**, 900 (2010).
[10] M. Mohseni, P. Rebentrost, S. Lloyd, and A. Aspuru-Guzik, J. Chem. Phys. **129**, 174106 (2008).
[11] S. Ballmann, R. Härtle, P. B. Coto, M. Elbing, M. Mayor, M. R. Bryce, M. Thoss, and H. B. Weber, Phys. Rev. Lett. **109**, 056801 (2012).
[12] F. H. L. Essler and R. M. Konik, Phys. Rev. B **78**, 100403 (2008).
[13] K. P. Schmidt and G. S. Uhrig, Phys. Rev. Lett. **90**, 227204 (2003).
[14] D. A. Tennant, B. Lake, A. J. A. James, F. H. L. Essler, S. Notbohm, H.-J. Mikeska, J. Fielden, P. Kögerler, P. C. Canfield, and M. T. F. Telling, Phys. Rev. B **85**, 014402 (2012).
[15] F. Groitl, T. Keller, K. Rolfs, D. A. Tennant, and K. Habicht, Phys. Rev. B **93**, 134404 (2016).
[16] A. J. A. James, F. H. L. Essler, and R. M. Konik, Phys. Rev. B **78**, 094411 (2008).
[17] A. James, Ph.D. thesis, University of Oxford, 2008.
[18] D. L. Quintero-Castro, B. Lake, A. T. M. N. Islam, E. M. Wheeler, C. Balz, M. Månsson, K. C. Rule, S. Gvasaliya, and A. Zheludev, Phys. Rev. Lett. **109**, 127206 (2012).
[19] J. Jensen, D. L. Quintero-Castro, A. T. M. N. Islam, K. C. Rule, M. Månsson, and B. Lake, Phys. Rev. B **89**, 134407 (2014).
[20] S. R. White, Phys. Rev. Lett. **69**, 2863 (1992).
[21] S. R. White, Phys. Rev. B **48**, 10345 (1993).
[22] U. Schollwöck, Ann. Phys. **326**, 96 (2011).
[23] B. Fauseweh, J. Stolze, and G. S. Uhrig, Phys. Rev. B **90**, 024428 (2014).
[24] B. Fauseweh and G. S. Uhrig, Phys. Rev. B **92**, 214417 (2015).
[25] Z. He, T. Kyômen, and M. Itoh, Phys. Rev. B **69**, 220407(R) (2004).
[26] H.-J. Koo and M.-H. Whangbo, Inorg. Chem. **45**, 4440 (2006).
[27] Y. Singh and D. C. Johnston, Phys. Rev. B **76**, 012407 (2007).
[28] D. C. Johnston, in *Handbook of Magnetic Materials*, edited by K. H. J. Buschow (Elsevier Science, Netherlands, 1997), Vol. 10.
[29] S. A. Zvyagin, J. Wosnitza, J. Krzystek, R. Stern, M. Jaime, Y. Sasago, and K. Uchinokura, Phys. Rev. B **73**, 094446 (2006).
[30] S. E. Sebastian, P. A. Sharma, M. Jaime, N. Harrison, V. Correa, L. Balicas, N. Kawashima, C. D. Batista, and I. R. Fisher, Phys. Rev. B **72**, 100404(R) (2005).
[31] S. E. Sebastian, Ph.D. thesis, Stanford University, 2006.
[32] J. C. Bonner, S. A. Friedberg, H. Kobayashi, D. L. Meier, and H. W. J. Blöte, Phys. Rev. B **27**, 248 (1983).
[33] K. Diederix, J. Groen, L. Henkens, T. Klaassen, and N. Poulis, Physica B **93**, 99 (1978).
[34] Z. He, T. Taniyama, and M. Itoh, J. Magn. Magn. Mater. **306**, 277 (2006).
[35] S. S. Salunke, A. V. Mahajan, and I. Dasgupta, Phys. Rev. B **77**, 012410 (2008).
[36] K. Ghoshray, B. Pahari, B. Bandyopadhyay, R. Sarkar, and A. Ghoshray, Phys. Rev. B **71**, 214401 (2005).
[37] C. S. Lue and B. X. Xie, Phys. Rev. B **72**, 052409 (2005).
[38] A. T. M. N. Islam, E. S. Klyushina, and B. Lake (unpublished).
[39] O. Sobolev and J. T. Park, J. Large Scale Res. Facil. **1**, A13 (2015).
[40] A. Weiße, G. Wellein, A. Alvermann, and H. Fehske, Rev. Mod. Phys. **78**, 275 (2006).
[41] A. Holzner, A. Weichselbaum, I. P. McCulloch, U. Schollwöck, and J. von Delft, Phys. Rev. B **83**, 195115 (2011).
[42] A. Braun and P. Schmitteckert, Phys. Rev. B **90**, 165112 (2014).
[43] F. A. Wolf, J. A. Justiniano, I. P. McCulloch, and U. Schollwöck, Phys. Rev. B **91**, 115144 (2015).
[44] A. C. Tiegel, S. R. Manmana, T. Pruschke, and A. Honecker, Phys. Rev. B **90**, 060406(R) (2014).
[45] A. C. Tiegel, A. Honecker, T. Pruschke, A. Ponomaryov, S. A. Zvyagin, R. Feyerherm, and S. R. Manmana, Phys. Rev. B **93**, 104411 (2016).
[46] See Supplemental Material at http://link.aps.org/supplemental/10.1103/PhysRevB.93.241109 for further details regarding to the fit analysis of the experimental data and for the description and comparison of the applied theoretical approaches.
[47] M. Ganahl, P. Thunström, F. Verstraete, K. Held, and H. G. Evertz, Phys. Rev. B **90**, 045144 (2014).
[48] F. A. Wolf, I. P. McCulloch, O. Parcollet, and U. Schollwöck, Phys. Rev. B **90**, 115124 (2014).
[49] S. Shamoto, M. Sato, J. M. Tranquada, B. J. Sternlieb, and G. Shirane, Phys. Rev. B **48**, 13817 (1993).
[50] T. Barnes, J. Riera, and D. A. Tennant, Phys. Rev. B **59**, 11384 (1999).
[51] C. Knetter and G. Uhrig, Eur. Phys. J. B **13**, 209 (2000).
[52] J. B. Goodenough, Phys. Rev. **117**, 1442 (1960).
[53] J. Kanamori, J. Phys. Chem. Solids **10**, 87 (1959).
[54] P. W. Anderson, Phys. Rev. **79**, 350 (1950).